

χ_{cJ} Polarization in Polarized Proton-Proton Collisions at RHIC

Gouranga C. Nayak¹

¹*22 West Fourth Street #1, Lewistown, Pennsylvania 17044, USA*

(Dated: September 4, 2018)

Abstract

We study inclusive χ_{cJ} production with definite polarizations in polarized proton-proton collisions at $\sqrt{s} = 200$ GeV and 500 GeV at RHIC by using non-relativistic QCD (NRQCD) color-octet mechanism. We present results of rapidity distribution of χ_{c0} , χ_{c1} and χ_{c2} production with specific polarizations in polarized p-p collisions at RHIC within the PHENIX detector acceptance range. We also present the corresponding results for the spin asymmetries.

PACS numbers: 12.38.Bx, 14.40.Lb, 13.85.Ni, 13.88+e

arXiv:1508.05850v2 [hep-ph] 17 Mar 2016

I. INTRODUCTION

RHIC (relativistic heavy ion collider) at BNL studies quark-gluon plasma in heavy-ion collisions and spin structure of the proton in polarized p-p collisions. The spin program at RHIC involves polarized proton collisions at $\sqrt{s}=200$ GeV and 500 GeV [1]. The quark-gluon plasma program involves Au-Au collisions at $\sqrt{s}=200$ GeV [2].

Measurements of heavy probes such as J/ψ , ψ' and χ_{cJ} are useful tools to detect quark-gluon plasma in heavy ion collisions and to extract polarized gluon distribution function inside proton in polarized p-p collisions [3, 4]. Hence it is necessary to analyze heavy quarkonium production mechanism in polarized p-p collisions at RHIC. Non-relativistic QCD (NRQCD) color-octet mechanism [5, 6] has been successful to study heavy quarkonium production at high energy colliders and at fixed target experiments.

The energy eigenstates of heavy quarkonium bound states $|H\rangle$ in NRQCD are labelled by the quantum numbers J^{PC} , with an additional superscript to give the color; (1) for singlet and (8) for octet. In the expansion of the Fock states the dominant component in S-wave orthoquarkonium is the pure quark-antiquark state $|Q\bar{Q}[{}^3S_1^{(1)}]\rangle$. The state, such as $|Q\bar{Q}[{}^3P_J^{(8)}]g\rangle$ with dynamical gluons contribute with a probability of order v^2 , where v is the typical velocity of the non-relativistic heavy quark (and antiquark), while the other states, such as $|Q\bar{Q}[{}^3S_1^{(1,8)}]gg\rangle$, $|Q\bar{Q}[{}^1S_0^{(8)}]g\rangle$ and $|Q\bar{Q}[{}^3D_J^{(1,8)}]gg\rangle$ contribute to the probability in higher orders in v . In P-wave orthoquarkonia, the dominant states are $|Q\bar{Q}[{}^3P_J^{(1)}]\rangle$ with the states having dynamical gluons such as $|Q\bar{Q}[{}^3S_1^{(8)}]g\rangle$ contribute with a probability of order v^2 . Once the $Q\bar{Q}$ is formed in a color octet state it may emit a soft gluon to transform into the color singlet state $|Q\bar{Q}[{}^3P_J^{(1)}]\rangle$ and become a J/ψ by photon decay. Also the $Q\bar{Q}$ pair in a color octet state can emit two long wavelength gluons to become J/ψ . These low energy interactions are negligible and the non-perturbative matrix elements, labelled by the above quantum numbers, can be extracted from experiments or can be calculated using lattice field theory.

NRQCD mechanism for heavy quarkonia production has been very successful in explaining data at high energy colliders such as in the p-p collisions at LHC [7], in the p- \bar{p} collisions at Tevatron [8–11], in the e-p collisions at HERA [12], in the e^+e^- collisions at LEP [13] and also at fixed target experiments [14]. The PHENIX data for J/ψ production in unpolarized p-p collisions can be explained by the NRQCD color octet mechanism [15].

In addition to unpolarized p-p collisions, RHIC offers a wide variety of measurements with respect to J/ψ production. They involve J/ψ production (with and without definite polarizations) in unpolarized p-p, d-Au, Cu-Cu and Au-Au collisions and in polarized p-p collisions. The parton fragmentation contribution to heavy quarkonium production will be very small at RHIC because the maximum transverse momentum of heavy quarkonium that can be measured at the RHIC is around 10 GeV/c. Hence we will neglect the parton fragmentation contribution to heavy quarkonium production in our study. We will focus on the main contributions to heavy quarkonium production at the RHIC which are from the parton fusion processes [15, 16].

In unpolarized and polarized partonic collisions, the inclusive heavy quarkonium production cross section (summed over quarkonium polarization states) were calculated in [10, 17] and [16, 18] respectively. Similarly, the heavy quarkonium production cross sections with definite polarizations in unpolarized partonic collisions were calculated in [19, 20]. At RHIC, the inclusive j/ψ and ψ' production with specific polarizations in polarized p-p collisions was studied in the PHENIX detector acceptance range in [21]. Similarly the double spin asymmetries in P-wave charmonium hadroproduction was considered for the first time in [22]. For earlier studies in the similar direction see [23].

In this paper we will study χ_{c0} , χ_{c1} and χ_{c2} polarizations in polarized p-p collisions at $\sqrt{s}=200$ GeV and 500 GeV at RHIC. The PHENIX collaborations at RHIC will study χ_{c0} , χ_{c1} and χ_{c2} polarizations in polarized p-p collisions at $\sqrt{s}=200$ GeV and 500 GeV [3].

We will evaluate the partonic level cross sections for the processes $q\bar{q}, gg \rightarrow \chi_{cJ}(\lambda)$ in polarized p-p collisions where λ is the helicity (polarization) of the heavy quarkonium state. Our LO analysis considers only the $\chi_{cJ}(\lambda)$ production in the forward direction at a finite rapidity. The reason we need these results is that the PHENIX collaboration at the RHIC will measure χ_{cJ} production with definite polarizations in polarized p-p collisions at $\sqrt{s} = 200$ GeV and 500 GeV. Since polarized heavy quarkonium production at the Tevatron energy scale [24] is not explained by the NRQCD color-octet mechanism [20] it will be useful to compare our results for χ_{cJ} polarizations with the future data at the RHIC. The study of polarized heavy quarkonium production in polarized p-p collisions at the RHIC is also unique in the sense that it probes the spin transfer processes in perturbative QCD (pQCD).

Note that the spin projection method [10] is normally used to evaluate the inclusive cross section for heavy quarkonium production (summed over polarization states) in parton fusion

processes. However, the heavy quarkonium production cross section with specific polarization in the final state can involve additional matrix elements that do not contribute when the polarization is summed. This involves interference terms between partonic processes that produce heavy quark-antiquark pairs with different total angular momenta. These interference terms cancel upon summing over polarizations. Such interference terms can be calculated by using the helicity decomposition method [19]. For this reason we will use the helicity decomposition method to calculate the square of the matrix elements for heavy quarkonium production with definite helicity in polarized partonic collisions. After evaluating the partonic level cross sections we will compute the rapidity distributions of the cross sections and spin asymmetries of χ_{c0} , χ_{c1} and χ_{c2} production with definite helicity states in polarized p-p collisions at RHIC at $\sqrt{s} = 200$ GeV and 500 GeV within the PHENIX detector acceptance ranges.

The paper is organized as follows. In section II we derive the partonic level cross sections for χ_{cJ} production with definite polarizations in polarized q- \bar{q} and g-g parton fusion processes using the helicity decomposition method within the NRQCD color-octet mechanism. In section III we present the results for the differential rapidity distributions and spin asymmetries for the $\chi_{cJ}(\lambda)$ in the PHENIX detector acceptance range in polarized p-p collisions at $\sqrt{s} = 200$ GeV and 500 GeV. We conclude in section IV.

II. INCLUSIVE χ_c PRODUCTION WITH DEFINITE HELICITIES IN POLARIZED PARTONIC COLLISIONS

In this section we will use the NRQCD color-octet mechanism and derive the square of the matrix element for inclusive χ_{cJ} production with definite helicities in polarized partonic fusion processes. We will consider the (polarized) partonic fusion processes $q\bar{q} \rightarrow \chi_{cJ}(\lambda)$ and $gg \rightarrow \chi_{cJ}(\lambda)$ where λ is the helicity of the produced heavy quarkonium state $H(\lambda)$. The helicity $\lambda = 0, \pm 1$ correspond to longitudinal and transverse polarization states respectively. As mentioned above, we will use the helicity decomposition method [19] within the NRQCD color-octet mechanism to calculate these processes where both initial and final state particles are polarized.

A. The $q\bar{q}$ fusion process

At the amplitude level the matrix element for the light quark-antiquark ($q\bar{q}$) fusion process $q(k_1) + \bar{q}(k_2) \rightarrow Q(p_1) + \bar{Q}(p_2)$ producing a heavy quark-antiquark ($Q\bar{Q}$) pair is given by

$$M_{q\bar{q} \rightarrow Q\bar{Q}} = \frac{g^2}{P^2} \bar{v}(k_2) \gamma_\mu T^a u(k_1) \bar{u}(p_1) \gamma^\mu T^a v(p_2), \quad (1)$$

where $P^\mu = p_1^\mu + p_2^\mu = k_1^\mu + k_2^\mu$ is the CM momentum of the pair and $p_1^\mu = P^\mu/2 + L_j^\mu q^j$ and $p_2^\mu = P^\mu/2 - L_j^\mu q^j$ with q^i being their relative momentum in the CM frame and L_j^μ is the boost matrix defined in [19] with both Lorentz and three vector indices. Using the non-relativistic heavy quark Pauli spinors (ξ and η) we obtain (up to terms linear in q):

$$|M_{q\bar{q} \rightarrow Q\bar{Q}}|^2 = \frac{g^4}{4m^2} \eta'^\dagger \sigma^i T^a \xi' L_i^\mu \bar{u}(k_1) \gamma_\mu T^a v(k_2) \bar{v}(k_2) \gamma_\nu T^b u(k_1) L_j^\nu \xi^\dagger \sigma^j T^b \eta, \quad (2)$$

where m is the mass of the heavy quark. We consider incoming (massless) light quarks and antiquarks

$$\begin{aligned} u(k_1) \bar{u}(k_1) &= \frac{1}{2} (1 + h_1 \gamma_5) \gamma_\mu k_1^\mu \\ v(k_2) \bar{v}(k_2) &= \frac{1}{2} (1 - h_2 \gamma_5) \gamma_\mu k_2^\mu \end{aligned} \quad (3)$$

where the polarized partonic matrix element squared involves the helicity combination $(+, +) - (+, -)$ with $+, -$ denoting the helicities h_1, h_2 of the incoming partons [21]. Then from eqs. (2) and (3) we find

$$\Delta |M_{q\bar{q} \rightarrow Q\bar{Q}}|^2 = \frac{g^4}{4m^2} \eta'^\dagger \sigma^i T^a \xi' \xi^\dagger \sigma^j T^a \eta [2m^2 n_i n_j - \delta_{ij} (k_1 \cdot k_2)], \quad (4)$$

using $(k_2 \cdot L)_i = -(k_1 \cdot L)_i = m n_i$ where n_i, n_j are the components of unit three-vectors $\mathbf{n}_1, \mathbf{n}_2$ which specify the polarizations of the heavy quarks and heavy antiquarks respectively in the charmonium bound state. The leading order term in an expansion in q gives

$$\Delta |M_{q\bar{q} \rightarrow Q\bar{Q}}|^2 = \frac{g^4}{4} [n_i n_j - \delta_{ij}] \eta'^\dagger \sigma^i T^a \xi' \xi^\dagger \sigma^j T^a \eta \quad (5)$$

which after averaging over the initial color (by dividing by 9) gives

$$\Delta |M_{q\bar{q} \rightarrow Q\bar{Q}}|^2 = \frac{4\pi^2 \alpha_s^2}{9} [n_i n_j - \delta_{ij}] \eta'^\dagger \sigma^i T^a \xi' \xi^\dagger \sigma^j T^a \eta. \quad (6)$$

As mentioned in the Appendix B in [19], the two-component spinor factors can be identified with various heavy quarkonium bound states $H(\lambda)$ with different quantum numbers

χ_{c0} Polarization in Unpolarized p-p Collisions at RHIC

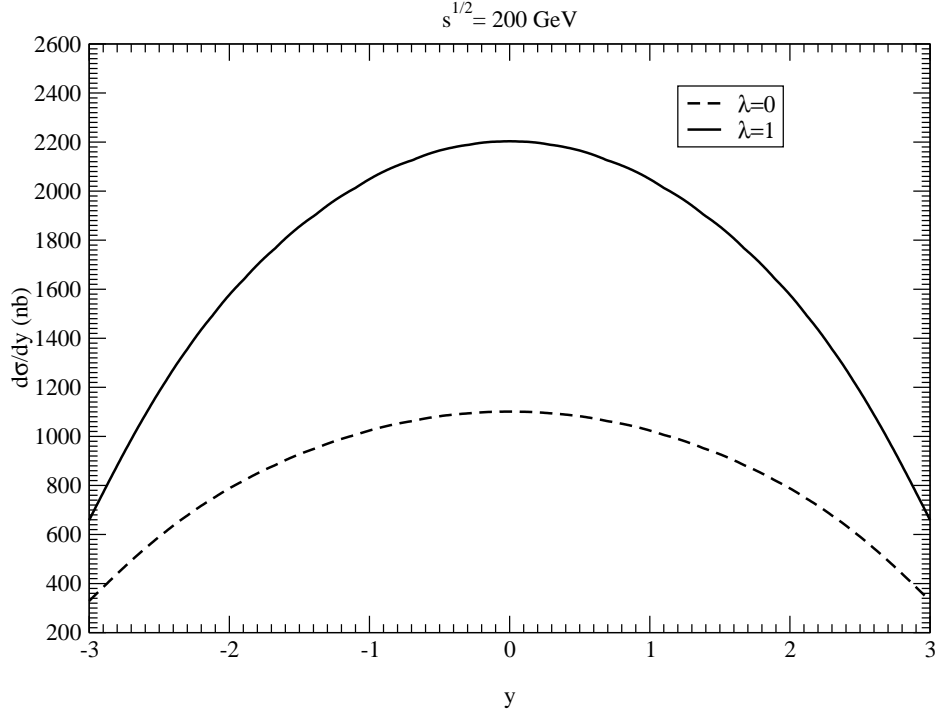


FIG. 1: Rapidity distribution of χ_{c0} production cross section at RHIC in pp collisions at $\sqrt{s} = 200 \text{ GeV}$.

as follows

$$\begin{aligned}
 4m^2 \eta^\dagger \xi' \xi^\dagger \eta &\equiv \langle \chi^\dagger \psi P_{H(\lambda)} \psi^\dagger \chi \rangle = \frac{4}{3} m \langle \mathcal{O}_1^H(1S_0) \rangle, \\
 4m^2 \eta^\dagger T^a \xi' \xi^\dagger T^a \eta &\equiv \langle \chi^\dagger T^a \psi P_{H(\lambda)} \psi^\dagger T^a \chi \rangle = \frac{4}{3} m \langle \mathcal{O}_8^H(1S_0) \rangle, \\
 4m^2 \eta^\dagger \sigma^i \xi' \xi^\dagger \sigma^j \eta &\equiv \langle \chi^\dagger \sigma^i \psi P_{H(\lambda)} \psi^\dagger \sigma^j \chi \rangle = \frac{4}{3} U_{\lambda i}^\dagger U_{j \lambda} m \langle \mathcal{O}_1^H(3S_1) \rangle, \\
 4m^2 \eta^\dagger \sigma^i T^a \xi' \xi^\dagger \sigma^j T^a \eta &\equiv \langle \chi^\dagger \sigma^i T^a \psi P_{H(\lambda)} \psi^\dagger \sigma^j T^a \chi \rangle = \frac{4}{3} U_{\lambda i}^\dagger U_{j \lambda} m \langle \mathcal{O}_8^H(3S_1) \rangle, \\
 4m^2 q^n q^m \eta^\dagger \sigma^i \xi' \xi^\dagger \sigma^j \eta &\equiv \langle \chi^\dagger (-\frac{i}{2} D^m) \sigma^i \psi P_{H(\lambda)} \psi^\dagger (-\frac{i}{2} D^n) \sigma^j \chi \rangle \\
 &= 4 U_{\lambda i}^\dagger U_{j \lambda} \delta^{mn} m \langle \mathcal{O}_1^H(3P_0) \rangle, \\
 4m^2 q^n q^m \eta^\dagger \sigma^i T^a \xi' \xi^\dagger \sigma^j T^a \eta &\equiv \langle \chi^\dagger (-\frac{i}{2} D^m) \sigma^i T^a \psi P_{H(\lambda)} \psi^\dagger (-\frac{i}{2} D^n) \sigma^j T^a \chi \rangle \\
 &= 4 U_{\lambda i}^\dagger U_{j \lambda} \delta^{mn} m \langle \mathcal{O}_8^H(3P_0) \rangle
 \end{aligned} \tag{7}$$

where

$$\sum_i U_{\lambda i} U_{i \lambda}^\dagger = 1$$

χ_{c0} Polarization in Polarized p-p Collisions at RHIC

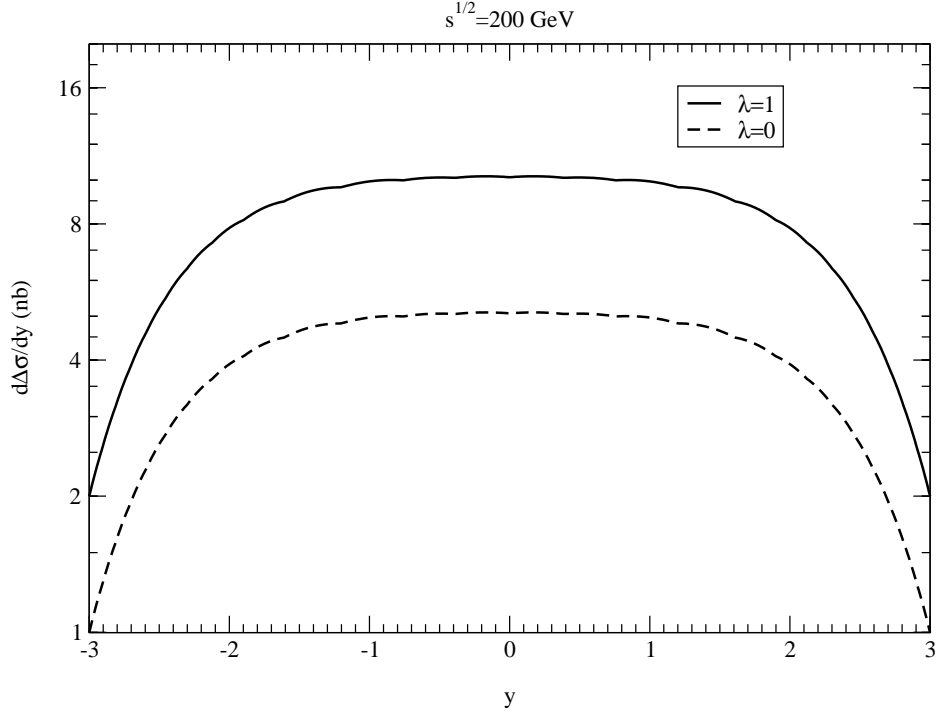


FIG. 2: Rapidity distribution of χ_{c0} production cross section at RHIC in polarized pp collisions at $\sqrt{s} = 200$ GeV.

$$\sum_i U_{\lambda i} n^i = \delta_{\lambda 0}, \quad (8)$$

where n^i is along the z-direction. Using the above equations we finally obtain

$$\Delta |M_{q\bar{q} \rightarrow H(\lambda)}|^2 = -\frac{4\pi^2 \alpha_s^2}{27} [1 - \delta_{\lambda 0}] \langle \mathcal{O}_8^H(^3S_1) \rangle. \quad (9)$$

The polarized quark-antiquark fusion process cross section for $\chi_c(\lambda)$ production is given by

$$\Delta \sigma_{q\bar{q} \rightarrow \chi_c(\lambda)} = -\delta(\hat{s} - 4m^2) \frac{\pi^3 \alpha_s^2}{27m^3} [1 - \delta_{\lambda 0}] \langle \mathcal{O}_8^{\chi_c}(^3S_1) \rangle \quad (10)$$

which vanishes for $\lambda = 0$.

B. The gg fusion process

At the amplitude level the matrix element for the gluon fusion process $g(k_1) + g(k_2) \rightarrow Q(p_1) + \bar{Q}(p_2)$ after including s, t, and u channel Feynman diagrams is given by

$$M_{gg \rightarrow Q\bar{Q}} = -g^2 \epsilon_\mu^a(k_1) \epsilon_\nu^{*b}(k_2) \left[\left(\frac{1}{6} \delta^{ab} + \frac{1}{2} d^{abc} T^c \right) S^{\mu\nu} + \frac{i}{2} f^{abc} T^c F^{\mu\nu} \right], \quad (11)$$

χ_{c0} Polarization in Unpolarized p-p Collisions at RHIC

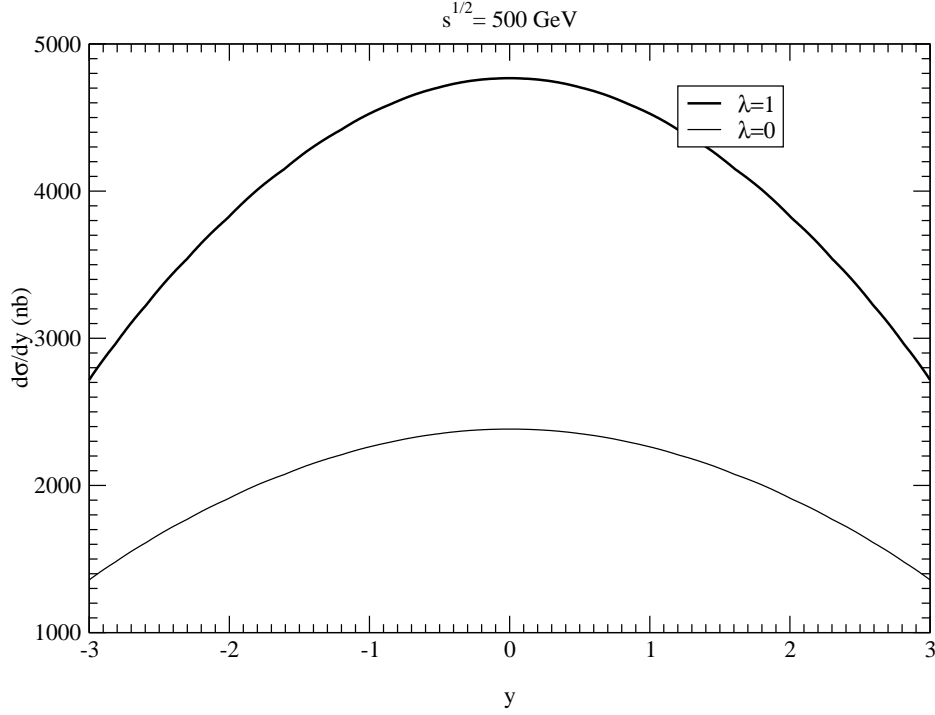


FIG. 3: Rapidity distribution of χ_{c0} production cross section at RHIC in pp collisions at $\sqrt{s} = 500$ GeV.

where

$$S^{\mu\nu} = \bar{u}(p_1) \left[\frac{\gamma^\mu (\not{p}_1 - \not{k}_1 + m) \gamma^\nu}{2p_1 \cdot k_1} + \frac{\gamma^\nu (\not{p}_1 - \not{k}_2 + m) \gamma^\mu}{2p_1 \cdot k_2} \right] v(p_2) \quad (12)$$

and

$$F^{\mu\nu} = \bar{u}(p_1) \left[\frac{\gamma^\mu (\not{p}_1 - \not{k}_1 + m) \gamma^\nu}{2p_1 \cdot k_1} - \frac{\gamma^\nu (\not{p}_1 - \not{k}_2 + m) \gamma^\mu}{2p_1 \cdot k_2} \right] \\ + \frac{2}{P^2} V^{\mu\nu\lambda}(k_1, k_2, -k_1 - k_2) \gamma_\lambda v(p_2) \quad (13)$$

where the three gluon vertex is denoted by $V^{\mu\nu\lambda}(k_1, k_2, k_3) = [(k_1 - k_2)^\lambda g^{\mu\nu} + (k_2 - k_3)^\mu g^{\nu\lambda} + (k_3 - k_1)^\nu g^{\lambda\mu}]$.

From the identities among the spinors and boost matrices from the appendix A of [19] we find

$$\bar{u}(p_1) \left[\frac{\gamma^\mu \not{k}_1 \gamma^\nu}{2p_1 \cdot k_1} + \frac{\gamma^\nu \not{k}_2 \gamma^\mu}{2p_1 \cdot k_2} \right] v(p_2) = \frac{i}{2m^2} (k_1 - k_2)_\lambda \epsilon^{\rho\mu\nu\lambda} P_\rho \xi^\dagger \eta \\ + \frac{(L \cdot k_1)_n}{m^3} [P^\nu L_j^\mu - P^\mu L_j^\nu + 2g^{\mu\nu} (L \cdot k_1)_j - (k_1 - k_2)^\mu L_j^\nu - (k_1 - k_2)^\nu L_j^\mu] q^n \xi^\dagger \sigma^j \eta \\ + \frac{(L \cdot k_1)_j}{m^3} [P^\mu L_n^\nu - P^\nu L_n^\mu] q^n \xi^\dagger \sigma^j \eta + \frac{1}{m} [P^\mu L_j^\nu - P^\nu L_j^\mu] \xi^\dagger \sigma^j \eta, \quad (14)$$

χ_{c0} Polarization in Polarized p-p Collisions at RHIC

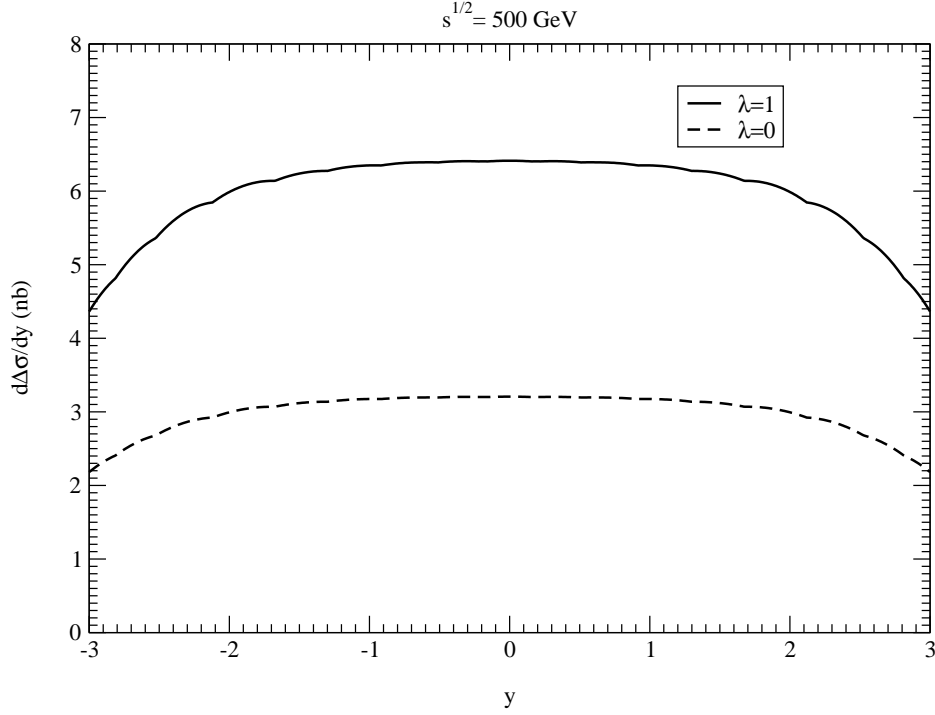


FIG. 4: Rapidity distribution of χ_{c0} production cross section at RHIC in polarized pp collisions at $\sqrt{s} = 500 \text{ GeV}$.

and

$$\begin{aligned}
 \bar{u}(p_1) \left[\frac{\gamma^\mu \not{k}_1 \gamma^\nu}{2p_1 \cdot k_1} - \frac{\gamma^\nu \not{k}_2 \gamma^\mu}{2p_1 \cdot k_2} \right] v(p_2) &= \frac{(L \cdot k_1)_n}{2m^4} (k_1 - k_2)_\lambda \epsilon^{\rho\mu\nu\lambda} P_\rho q^n \xi^\dagger \eta \\
 &- \frac{(L \cdot k_1)_n}{m^3} [P^\nu L_j^\mu + P^\mu L_j^\nu] q^n \xi^\dagger \sigma^j \eta \\
 &- \frac{1}{m} [2g^{\mu\nu} (L \cdot k_1)_j - (k_1 - k_2)^\mu L_j^\nu - (k_1 - k_2)^\nu L_j^\mu] \xi^\dagger \sigma^j \eta \\
 &+ \frac{2}{m} [L_n^\mu L_j^\nu - L_n^\nu L_j^\mu] q^n \xi^\dagger \sigma^j \eta.
 \end{aligned} \tag{15}$$

Using above equations we find

$$\begin{aligned}
 S^{\mu\nu} &= \frac{i}{2m^2} (k_1 - k_2)_\lambda \epsilon^{\rho\mu\nu\lambda} P_\rho \xi^\dagger \eta + \left[\frac{(L \cdot k_1)_j}{m^3} (P^\nu L_n^\mu - P^\mu L_n^\nu - 2g^{\mu\nu} (L \cdot k_1)_n) \right. \\
 &+ \left. \frac{2}{m} [L_n^\mu L_j^\nu + L_n^\nu L_j^\mu] + \frac{1}{m^3} (L \cdot k_1)_n [(k_1 - k_2)^\mu L_j^\nu + (k_1 - k_2)^\nu L_j^\mu] \right] q^n \xi^\dagger \sigma^j \eta,
 \end{aligned} \tag{16}$$

and

$$F^{\mu\nu} = \frac{i(L \cdot k_1)_n}{2m^4} (k_1 - k_2)_\lambda \epsilon^{\rho\mu\nu\lambda} P_\rho q^n \xi^\dagger \eta + [k_2^\nu L_j^\mu - k_1^\mu L_j^\nu] \xi^\dagger \sigma^j \eta. \tag{17}$$

χ_{c1} Polarization in Unpolarized p-p Collisions at RHIC

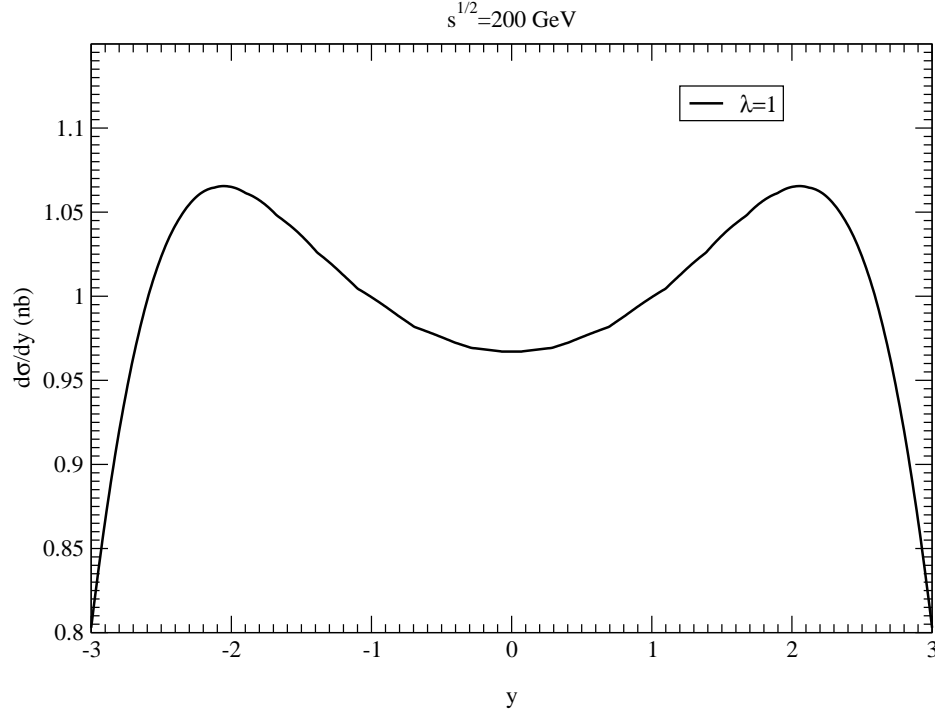


FIG. 5: Rapidity distribution of χ_{c1} production cross section at RHIC in pp collisions at $\sqrt{s} = 200 \text{ GeV}$.

The square of gluon polarization vector, for an incoming gluon with a helicity λ_i , can be written as [25]

$$\epsilon_\mu^a(k_1, \lambda_i) \epsilon_\nu^{*b}(k_1, \lambda_i) = \frac{1}{2} \delta^{ab} \left[-g_{\mu\nu} + \frac{k_{1\mu} k_{2\nu} + k_{2\mu} k_{1\nu}}{k_1 \cdot k_2} - i \lambda_i \epsilon_{\mu\nu\rho\delta} \frac{k_1^\rho k_2^\delta}{k_1 \cdot k_2} \right]. \quad (18)$$

Choosing longitudinally polarized gluons and using the relation

$$\epsilon_{\mu\mu'\alpha\beta} k_1^\alpha k_2^\beta = 2m^2 \epsilon^{ijk} n_k L_i^\mu L_j^\nu, \quad (19)$$

from appendix A of [19] we find that

$$\begin{aligned} \Delta |M_{gg \rightarrow Q\bar{Q}}|^2 &= -\frac{g^4}{4} \epsilon^{pqr} \epsilon^{p'q'r'} n_r n_{r'} \\ &\times [S^{ab} S^{*ab} L_{\mu p} L_{\nu p'} S^{\mu\nu} L_{\mu' q} L_{\nu' q'} S^{*\mu'\nu'} + F^{ab} F^{*ab} L_{\mu p} L_{\nu p'} F^{\mu\nu} L_{\mu' q} L_{\nu' q'} F^{*\mu'\nu'}], \end{aligned} \quad (20)$$

where

$$S^{ab} = \frac{1}{6} \delta^{ab} + \frac{1}{2} d^{abc} T^c \quad \text{and} \quad F^{ab} = \frac{i}{2} f^{abc} T^c. \quad (21)$$

χ_{c1} Polarization in Polarized p-p Collisions at RHIC

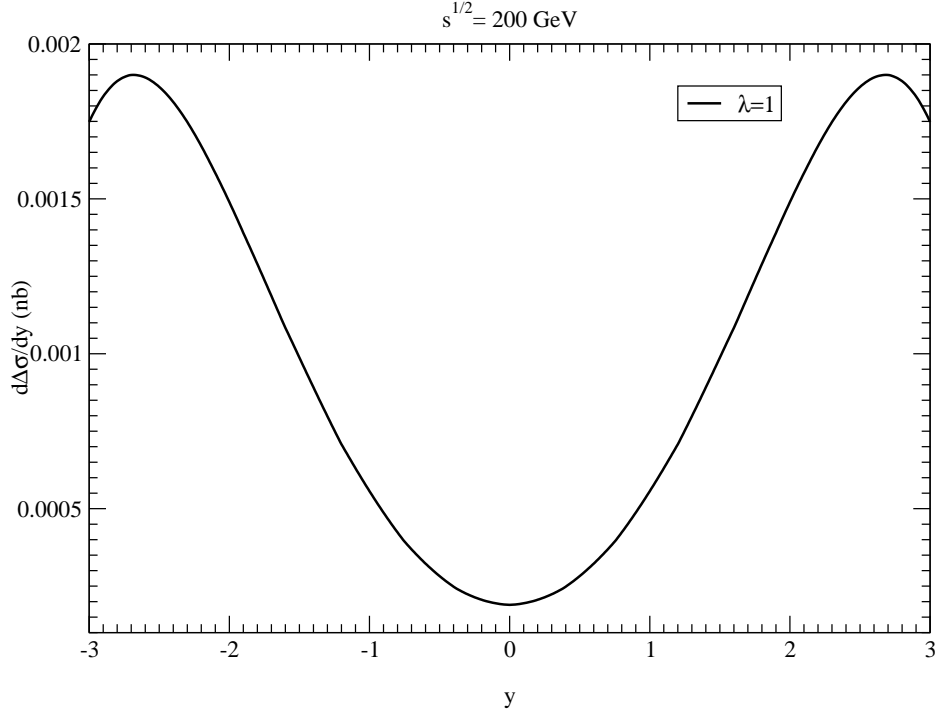


FIG. 6: Rapidity distribution of χ_{c1} production cross section at RHIC in polarized pp collisions at $\sqrt{s} = 200 \text{ GeV}$.

Using the properties of L_i^μ matrices [19] and after averaging over the initial color (by dividing by 64) we find

$$\begin{aligned}
 \Delta |M_{gg \rightarrow Q\bar{Q}}|^2 = & -\frac{\pi^2 \alpha_s^2}{9} [\eta^\dagger \xi' \xi^\dagger \eta + \frac{1}{m^2} [(n \cdot q) n_j q_{j'} + (n \cdot q') n_{j'} q_j - \frac{3}{2} (n \cdot q) (n \cdot q') n_j n_{j'} \\
 & - (n \times q')_j (n \times q)_{j'}] \eta^\dagger \sigma^{j'} \xi' \xi^\dagger \sigma^j \eta + \frac{15}{8} \eta^\dagger T^a \xi' \xi^\dagger T^a \eta + \frac{15}{8m^2} [(n \cdot q) n_j q_{j'} + (n \cdot q') n_{j'} q_j \\
 & - \frac{3}{2} (n \cdot q) (n \cdot q') n_j n_{j'} - (n \times q')_j (n \times q)_{j'}] \eta^\dagger \sigma^{j'} T^a \xi' \xi^\dagger \sigma^j T^a \eta \\
 & + \frac{27}{8m^2} (n \cdot q) (n \cdot q') \eta^\dagger T^a \xi' \xi^\dagger T^a \eta]. \tag{22}
 \end{aligned}$$

While for j/ψ and ψ' production the matrix elements $\langle \mathcal{O}_8^{j/\psi(\psi')}({}^1S_0) \rangle$, $\langle \mathcal{O}_8^{j/\psi(\psi')}({}^3S_1) \rangle$ and $\langle \mathcal{O}_8^{j/\psi(\psi')}({}^3P_0) \rangle$ are important [21], for χ_{c0} production the matrix elements $\langle \mathcal{O}_8^{\chi_{c0}}({}^3S_1) \rangle$ and $\langle \mathcal{O}_1^{\chi_{c0}}({}^3P_0) \rangle$ are important [26].

We identify different bound states as given in eq. (7) and use eq. (8) to obtain

$$\Delta \sigma_{gg \rightarrow \chi_0(\lambda)} = -\delta(\hat{s} - 4m^2) \frac{\pi^3 \alpha_s^2}{36m^5} \left(\frac{1}{2} \delta_{\lambda 0} - 1 \right) \langle \mathcal{O}_1^{\chi_{c0}}({}^3P_0) \rangle. \tag{23}$$

χ_{c1} Polarization in Unpolarized p-p Collisions at RHIC

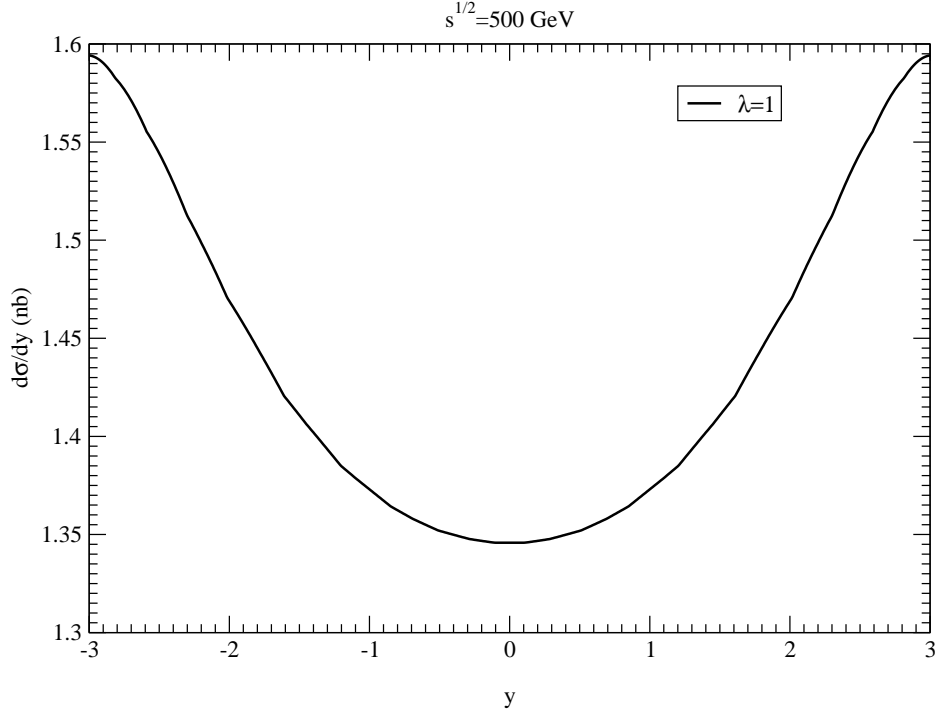


FIG. 7: Rapidity distribution of χ_{c1} production cross section at RHIC in pp collisions at $\sqrt{s} = 500$ GeV.

and

$$\Delta\sigma_{gg\rightarrow\chi_2(\lambda)} = -\delta(\hat{s} - 4m^2) \frac{\pi^3\alpha_s^2}{135m^5} \left(\frac{1}{2}\delta_{\lambda 0} - 1\right) \langle \mathcal{O}_1^{\chi_{c2}}(^3P_2) \rangle. \quad (24)$$

C. The Polarized Proton-Proton Collisions

Folding eqs. (10), (23) with parton densities we find the following cross section for $\chi_{c0}(\lambda)$ in longitudinally polarized proton-proton collisions

$$\begin{aligned} \Delta\sigma_{(pp\rightarrow\chi_{c0}(\lambda))} &= \frac{\pi^3\alpha_s^2}{27sm^3} \int_{4m^2/s}^1 \frac{dx_1}{x_1} [\Delta f_q(x_1, 2m) \Delta f_{\bar{q}}\left(\frac{4m^2}{x_1 s}, 2m\right) \\ &\times (\delta_{\lambda 0} - 1) \langle \mathcal{O}_8^{\chi_{c0}}(^3S_1) \rangle + \frac{1}{4} \Delta f_g(x_1, 2m) \Delta f_g\left(\frac{4m^2}{x_1 s}, 2m\right) \\ &\times \frac{9}{m^2} (1 - \frac{1}{2}\delta_{\lambda 0}) \langle \mathcal{O}_1^{\chi_{c0}}(^3P_0) \rangle], \end{aligned} \quad (25)$$

where $\Delta f(x, Q)$ ($\Delta g(x, Q)$) denote the polarized quark (gluon) distribution functions inside the proton at the scale Q .

χ_{c1} Polarization in Polarized p-p Collisions at RHIC

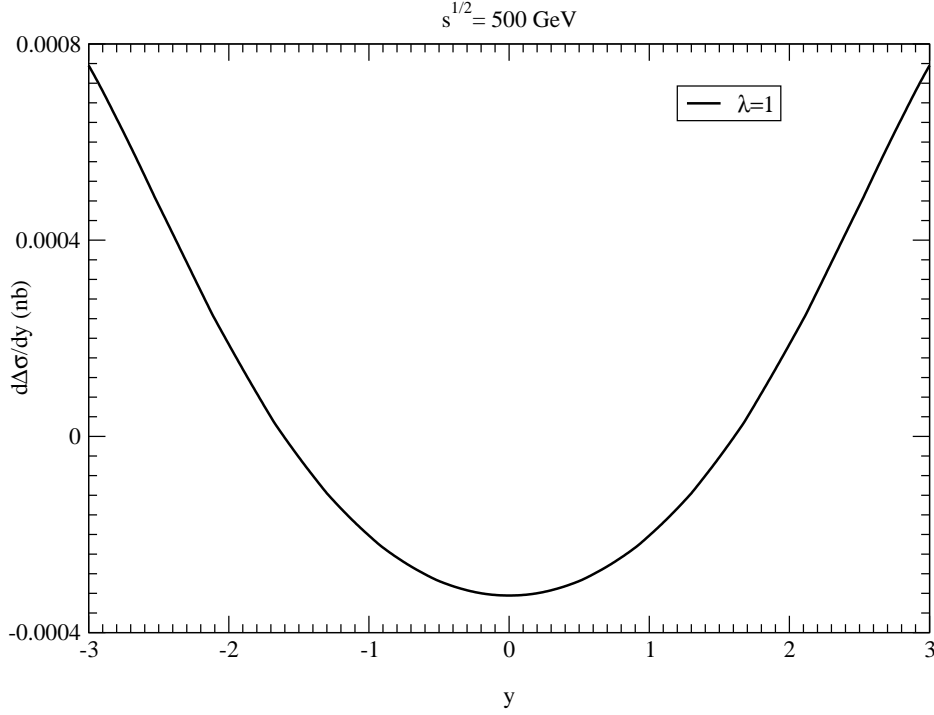


FIG. 8: Rapidity distribution of χ_{c1} production cross section at RHIC in polarized pp collisions at $\sqrt{s} = 500 \text{ GeV}$.

Folding eqs. (10) with parton densities we find the following cross section for $\chi_{c1}(\lambda)$ in longitudinally polarized proton-proton collisions

$$\begin{aligned} \Delta\sigma_{(pp \rightarrow \chi_{c1}(\lambda))} &= \frac{\pi^3 \alpha_s^2}{27 s m^3} \int_{4m^2/s}^1 \frac{dx_1}{x_1} [\Delta f_q(x_1, 2m) \Delta f_{\bar{q}}(\frac{4m^2}{x_1 s}, 2m) \\ &\times (\delta_{\lambda 0} - 1) \langle \mathcal{O}_8^{\chi_{c1}}(^3S_1) \rangle], \end{aligned} \quad (26)$$

Similarly, folding eqs. (10), (24) with parton densities we find the following cross section for $\chi_{c2}(\lambda)$ in longitudinally polarized proton-proton collisions

$$\begin{aligned} \Delta\sigma_{(pp \rightarrow \chi_{c2}(\lambda))} &= \frac{\pi^3 \alpha_s^2}{27 s m^3} \int_{4m^2/s}^1 \frac{dx_1}{x_1} [\Delta f_q(x_1, 2m) \Delta f_{\bar{q}}(\frac{4m^2}{x_1 s}, 2m) \\ &\times (\delta_{\lambda 0} - 1) \langle \mathcal{O}_8^{\chi_{c2}}(^3S_1) \rangle + \frac{1}{15} \Delta f_g(x_1, 2m) \Delta f_g(\frac{4m^2}{x_1 s}, 2m) \\ &\times \frac{9}{m^2} (1 - \frac{1}{2} \delta_{\lambda 0}) \langle \mathcal{O}_1^{\chi_{c2}}(^3P_2) \rangle], \end{aligned} \quad (27)$$

The corresponding production cross sections for unpolarized proton-proton collisions are [19]:

$$\sigma_{(pp \rightarrow \chi_0(\lambda))} = \frac{\pi^3 \alpha_s^2}{27 s m^3} \int_{4m^2/s}^1 \frac{dx_1}{x_1} [f_q(x_1, 2m) f_{\bar{q}}(\frac{4m^2}{x_1 s}, 2m)$$

χ_{c2} Polarization in Unpolarized p-p Collisions at RHIC

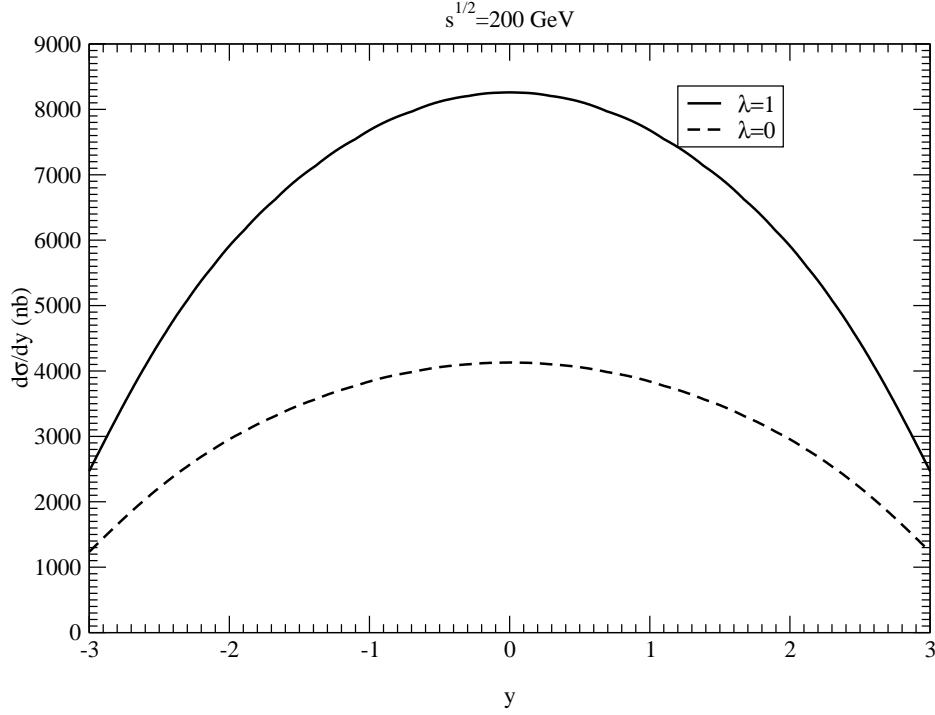


FIG. 9: Rapidity distribution of χ_{c2} production cross section at RHIC in pp collisions at $\sqrt{s} = 200 \text{ GeV}$.

$$\begin{aligned}
 & \times (1 - \delta_{\lambda 0}) \langle \mathcal{O}_8^{\chi_{c0}}(^3S_1) \rangle + \frac{1}{4} f_g(x_1, 2m) f_g\left(\frac{4m^2}{x_1 s}, 2m\right) \\
 & \times \frac{9}{m^2} \left(1 - \frac{2}{3} \delta_{\lambda 0}\right) \langle \mathcal{O}_1^{\chi_{c0}}(^3P_0) \rangle, \tag{28}
 \end{aligned}$$

$$\begin{aligned}
 \sigma_{(pp \rightarrow \chi_1(\lambda))} &= \frac{\pi^3 \alpha_s^2}{27 s m^3} \int_{4m^2/s}^1 \frac{dx_1}{x_1} [f_q(x_1, 2m) f_{\bar{q}}\left(\frac{4m^2}{x_1 s}, 2m\right) \\
 & \times (1 - \delta_{\lambda 0}) \langle \mathcal{O}_8^{\chi_{c1}}(^3S_1) \rangle] \tag{29}
 \end{aligned}$$

and

$$\begin{aligned}
 \sigma_{(pp \rightarrow \chi_2(\lambda))} &= \frac{\pi^3 \alpha_s^2}{27 s m^3} \int_{4m^2/s}^1 \frac{dx_1}{x_1} [f_q(x_1, 2m) f_{\bar{q}}\left(\frac{4m^2}{x_1 s}, 2m\right) \\
 & \times (1 - \delta_{\lambda 0}) \langle \mathcal{O}_8^{\chi_{c2}}(^3S_1) \rangle + \frac{1}{15} f_g(x_1, 2m) f_g\left(\frac{4m^2}{x_1 s}, 2m\right) \\
 & \times \frac{9}{m^2} \left(1 - \frac{2}{3} \delta_{\lambda 0}\right) \langle \mathcal{O}_1^{\chi_{c2}}(^3P_0) \rangle]. \tag{30}
 \end{aligned}$$

The spin asymmetry $A_{LL}(\lambda)$ is given by the ratio of the above cross sections

$$A_{LL}(\lambda) = \frac{d\Delta\sigma(\lambda)}{d\sigma(\lambda)}. \tag{31}$$

χ_{c2} Polarization in Polarized p-p Collisions at RHIC

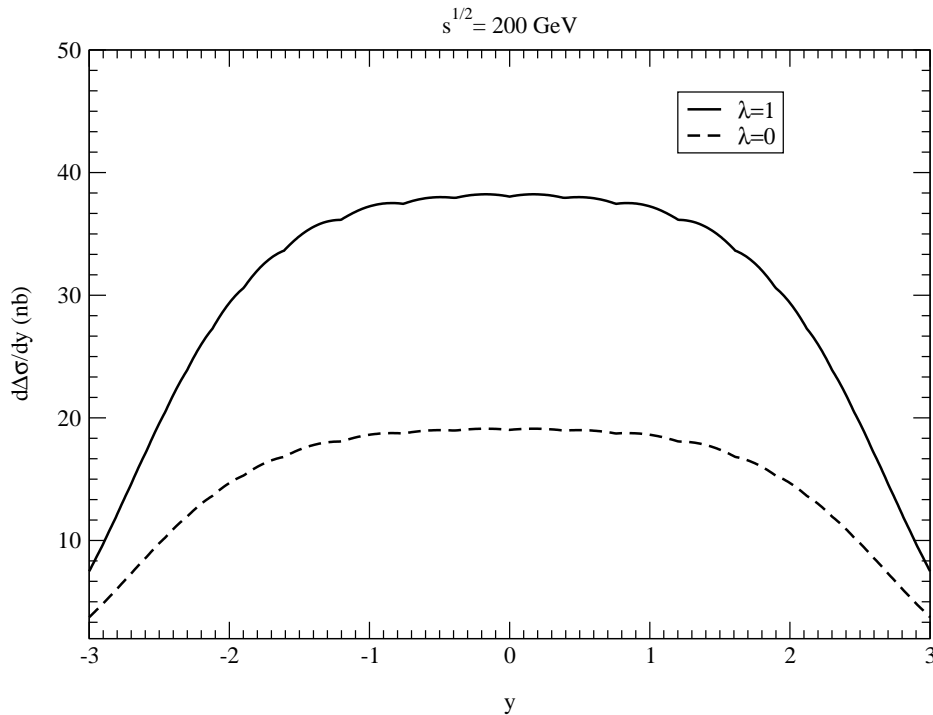


FIG. 10: Rapidity distribution of χ_{c2} production cross section at RHIC in polarized pp collisions at $\sqrt{s} = 200 \text{ GeV}$.

III. RESULTS AND DISCUSSION

In this section, using the formulae derived above, we compute the LO rapidity distributions and spin asymmetries for the heavy charmonium systems χ_{cJ} in longitudinally polarized proton-proton collisions at RHIC. We present the results for the χ_{c0} , χ_{c1} and χ_{c2} production with definite polarizations in unpolarized as well as polarized proton-proton collisions at $\sqrt{s} = 200 \text{ GeV}$ and 500 GeV at RHIC. These results provide interesting information on the polarization state of these heavy charmonium states.

We use the following values for the NRQCD non-perturbative matrix elements. From the Fermilab Tevatron, see [27] and [10], the central values for χ_{cJ} production the non-perturbative matrix elements are given by [11]

$$\langle \mathcal{O}_8^{\chi_{c0}}(^3S_1) \rangle = 0.0019 \text{ GeV}^3, \quad \langle \mathcal{O}_1^{\chi_{c0}}(^3P_0) \rangle = 0.089 \text{ GeV}^5. \quad (32)$$

The non-perturbative matrix elements for χ_{c1} and χ_{c2} can be obtained by using symmetry

χ_{c2} Polarization in Unpolarized p-p Collisions at RHIC

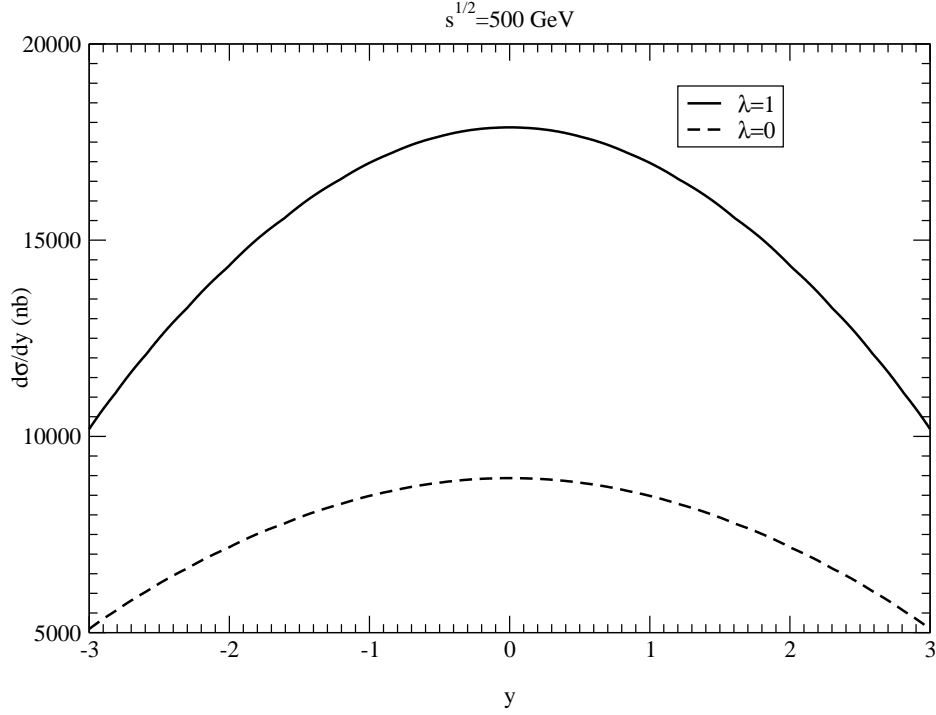


FIG. 11: Rapidity distribution of χ_{c2} production cross section at RHIC in pp collisions at $\sqrt{s} = 500$ GeV.

as follows

$$\langle \mathcal{O}_8^{\chi_{cJ}}(^3S_1) \rangle = (2J + 1) \langle \mathcal{O}_8^{\chi_{c0}}(^3S_1) \rangle, \quad \langle \mathcal{O}_1^{\chi_{cJ}}(^3P_J) \rangle = (2J + 1) \langle \mathcal{O}_1^{\chi_{c0}}(^3P_0) \rangle. \quad (33)$$

A. Rapidity Distribution of χ_{cJ} Cross Sections at RHIC

We will present our results in the rapidity range $-3 < y < 3$. This covers the central arm (forward arm) electron (muon) detector at the PHENIX experiment for the χ_{cJ} rapidity range $-0.5 < y < 0.5$ ($1 < |y| < 2$). We will present our differential rapidity distributions and spin asymmetries for χ_{cJ} production with helicities $\lambda = 1$ and 0 in unpolarized and polarized p-p collisions at $\sqrt{s} = 200$ GeV and 500 GeV in the above detector acceptance ranges.

We take the charm quark mass $m=1.5$ GeV and the mass factorization scale equal to $2m$. Several groups have produced polarized parton density sets [29],[30] and [31]. We choose

χ_{c2} Polarization in Polarized p-p Collisions at RHIC

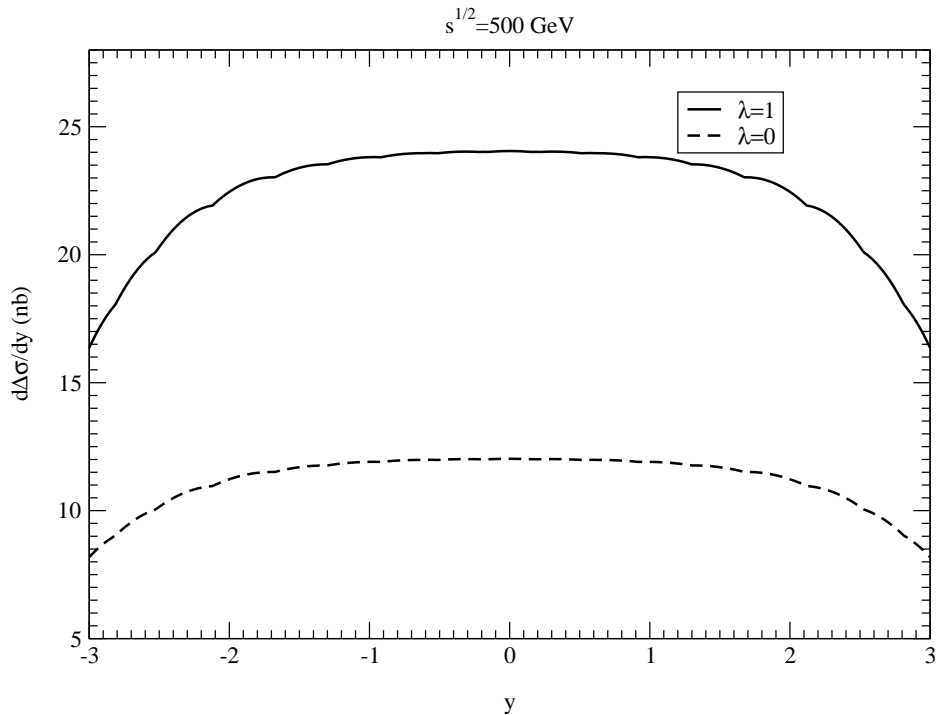


FIG. 12: Rapidity distribution of χ_{c2} production cross section at RHIC in polarized pp collisions at $\sqrt{s} = 500$ GeV.

the GRV unpolarized LO parton densities [32] and the GRSV [30] polarized densities. The latter authors have a standard scenario and a valence scenario. For simplicity we choose the former. Therefore we always use the LO four flavour sets (for the u, d, s and g partons) and we set $n_f = 4$ in the one-loop running coupling constant and the parton densities. For both parton density sets we use $\Lambda_4^{\text{LO}} = 175$ MeV, so that $\alpha_s^{\text{LO}}(m_Z) = 0.121$ at the mass of the Z.

In Fig. 1 we present the rapidity differential distributions for χ_{c0} production in unpolarized p-p collisions at $\sqrt{s} = 200$ GeV. The solid and dashed lines correspond to $\lambda=1$ and 0 respectively. Note that for $\lambda=0$ the cross section becomes small because the color octet contribution from the quark-antiquark process at LO vanishes, see eq. (28). The color singlet contribution is from gluon fusion process at LO, see eq. (28).

In Fig. 2 we present the rapidity differential distributions for χ_{c0} production in polarized p-p collisions at $\sqrt{s} = 200$ GeV. The solid and dashed lines correspond to $\lambda=1$ and 0 respectively. Note that for $\lambda=0$ the cross section becomes small because the color octet contribution from the quark-antiquark process at LO vanishes, see eq. (10). The color

singlet contribution is from gluon fusion process at LO, see eq. (25).

In Fig. 3 we present the rapidity differential distributions for χ_{c0} production in unpolarized p-p collisions at $\sqrt{s} = 500$ GeV. The solid and dashed lines correspond to $\lambda=1$ and 0 respectively. We find that the cross section for χ_{c0} production in unpolarized p-p collisions at $\sqrt{s}=500$ GeV is larger than that at $\sqrt{s}=200$ GeV. This is due to the enhancement of parton distribution function.

In Fig. 4 we present the rapidity differential distributions for χ_{c0} production in polarized p-p collisions at $\sqrt{s} = 500$ GeV. The solid and dashed lines correspond to $\lambda=1$ and 0 respectively. We find that the cross section for χ_{c0} production in polarized p-p collisions at $\sqrt{s}=500$ GeV is smaller than that at $\sqrt{s}=200$ GeV. This is due to the polarized parton distribution function.

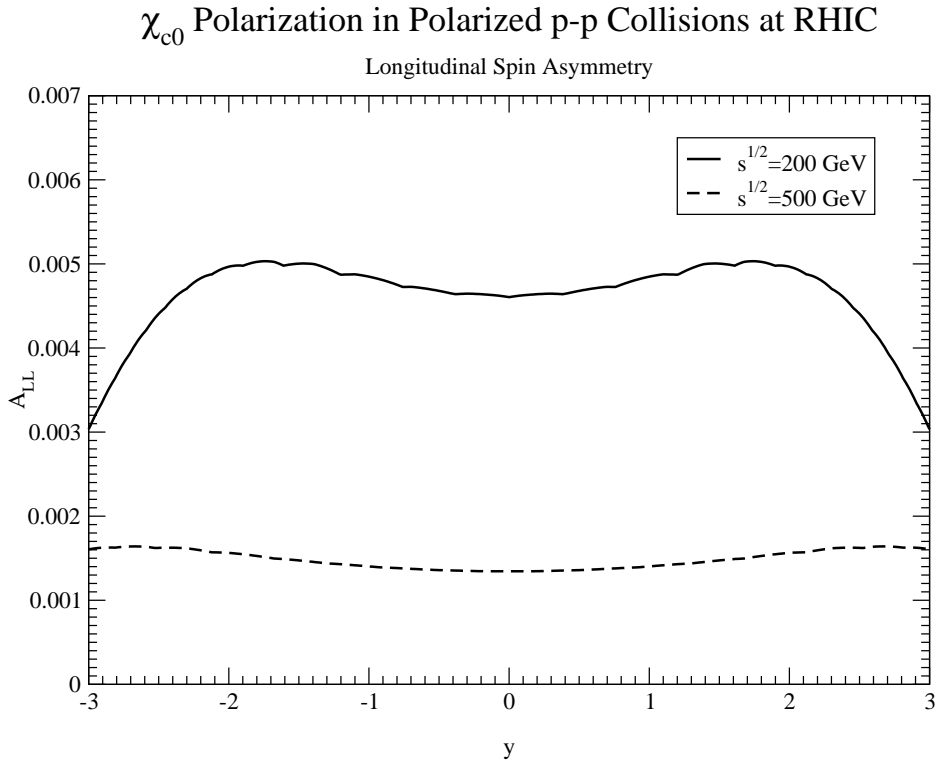


FIG. 13: Rapidity distribution of longitudinal spin asymmetry A_{LL} of χ_{c0} production at RHIC in polarized pp collisions.

In Fig. 5 we present the rapidity differential distributions for χ_{c1} production in unpolarized p-p collisions at $\sqrt{s} = 200$ GeV. Note that the shape of the curve is different than that from χ_{c0} production because the contribution to χ_{c1} production is from quark-antiquark fu-

sion process via color octet mechanism. At LO the gluon fusion process in the color singlet channel does not contribute to the χ_{c1} production, see eq. (29).

In Fig. 6 we present the rapidity differential distributions for χ_{c1} production in polarized p-p collisions at $\sqrt{s} = 200$ GeV. In case of χ_{c1} production the $\lambda=1$ contributes because for $\lambda=0$ the cross section in eq. (10) in polarized p-p collisions vanishes. At LO the gluon fusion process in the color singlet channel does not contribute to the χ_{c1} production in polarized p-p collisions, see eq. (26).

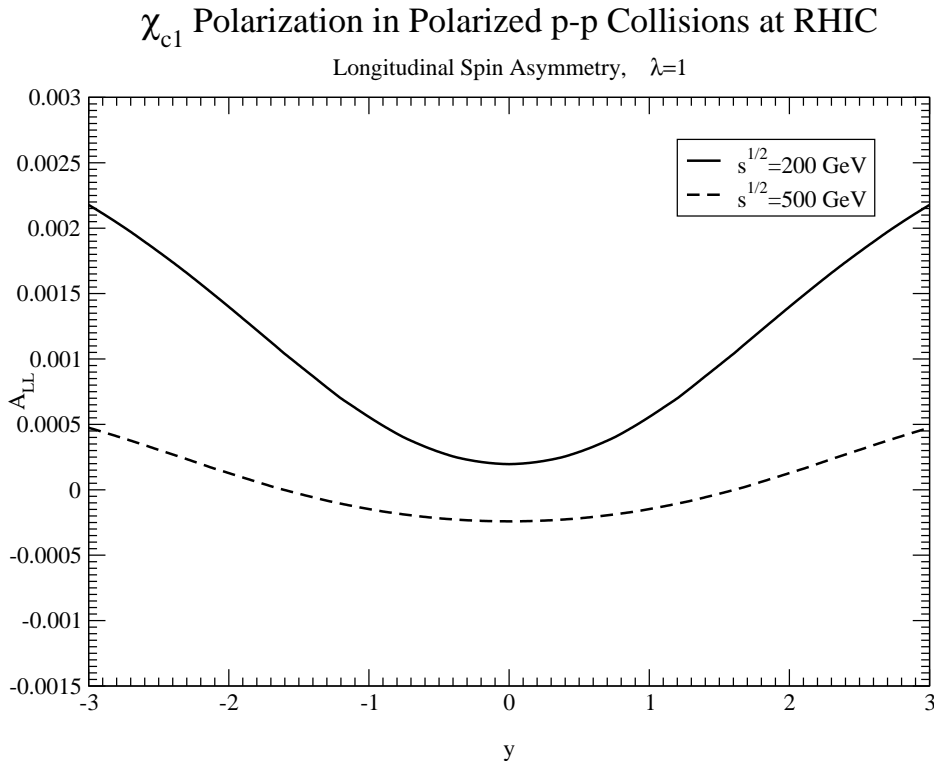


FIG. 14: Rapidity distribution of longitudinal spin asymmetry A_{LL} of χ_{c1} production at RHIC in polarized pp collisions.

In Fig. 7 we present the rapidity differential distributions for χ_{c1} production in unpolarized p-p collisions at $\sqrt{s} = 500$ GeV. We find that the cross section for χ_{c1} production in unpolarized p-p collisions at $\sqrt{s}=500$ GeV is larger than that at $\sqrt{s}=200$ GeV. This is due to the enhancement of parton distribution function.

In Fig. 8 we present the rapidity differential distributions for χ_{c1} production in polarized p-p collisions at $\sqrt{s} = 500$ GeV. Note that the values in some rapidity ranges become negative which is due to the polarized quark distribution function at this center of mass energy. We

find that the cross section for χ_{c1} production in polarized p-p collisions at $\sqrt{s}=500$ GeV is smaller than that at $\sqrt{s}=200$ GeV. This is due to the polarized parton distribution function.

In Fig. 9 we present the rapidity differential distributions for χ_{c2} production in unpolarized p-p collisions at $\sqrt{s} = 200$ GeV. The solid and dashed lines correspond to $\lambda=1$ and 0 respectively. Note that for $\lambda=0$ the cross section becomes small because the color octet contribution vanishes, see eq. (30). The color singlet contribution is from gluon fusion process at LO, see eq. (30).

In Fig. 10 we present the rapidity differential distributions for χ_{c2} production in polarized p-p collisions at $\sqrt{s} = 200$ GeV. The solid and dashed lines correspond to $\lambda=1$ and 0 respectively. For $\lambda=0$ the cross section becomes small because the color octet contribution vanishes, see eq. (10). The color singlet contribution is from gluon fusion process at LO, see eq. (27).

In Fig. 11 we present the rapidity differential distributions for χ_{c2} production in unpolarized p-p collisions at $\sqrt{s} = 500$ GeV. The solid and dashed lines correspond to $\lambda=1$ and 0 respectively. We find that the cross section for χ_{c2} production in unpolarized p-p collisions at $\sqrt{s}=500$ GeV is larger than that at $\sqrt{s}=200$ GeV. This is due to the enhancement of parton distribution function.

In Fig. 12 we present the rapidity differential distributions for χ_{c2} production in polarized p-p collisions at $\sqrt{s} = 500$ GeV. The solid and dashed lines correspond to $\lambda=1$ and 0 respectively. We find that the cross section for χ_{c2} production in polarized p-p collisions at $\sqrt{s}=500$ GeV is smaller than that at $\sqrt{s}=200$ GeV. This is due to the polarized parton distribution function.

B. Spin Asymmetry of χ_c at RHIC

In Fig. 13 we present the rapidity distributions of the longitudinal spin asymmetry A_{LL} for χ_{c0} production in polarized p-p collisions at RHIC. The solid line is for $\sqrt{s}=200$ GeV polarized pp collisions and the dashed line is for $\sqrt{s}=500$ GeV polarized pp collisions. Note that the spin asymmetry is decreased for higher energies. The spin asymmetry for χ_{c0} production is almost same for $\lambda=1$ and 0.

In Fig. 14 we present the rapidity distributions of the longitudinal spin asymmetry A_{LL} for χ_{c1} production in polarized p-p collisions at RHIC. The solid line is for $\sqrt{s}=200$ GeV

χ_{c2} Polarization in Polarized p-p Collisions at RHIC

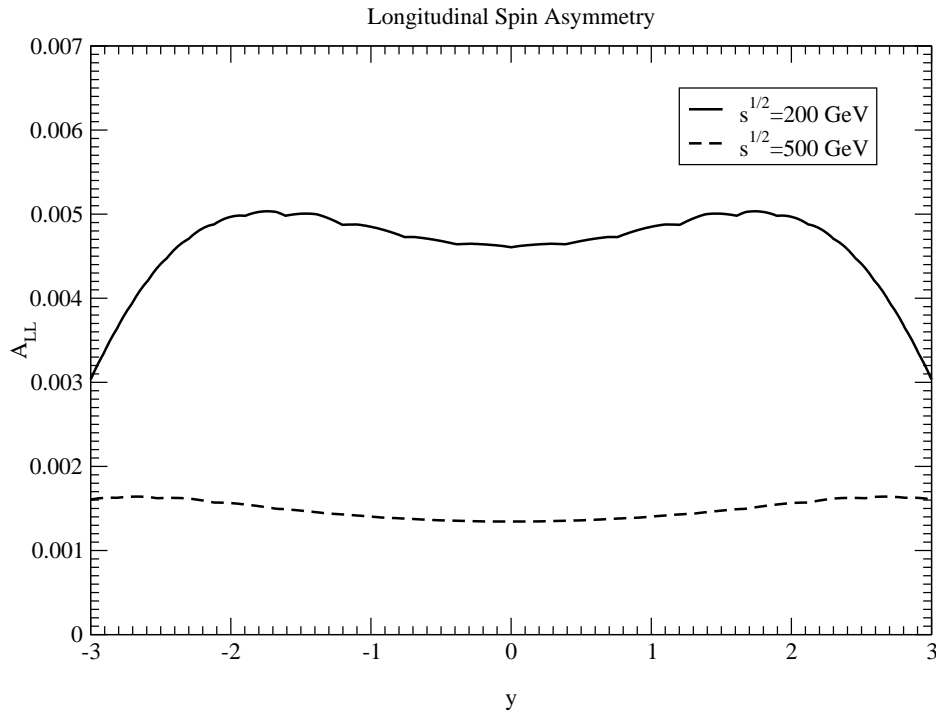


FIG. 15: Rapidity distribution of longitudinal spin asymmetry A_{LL} of χ_{c2} production at RHIC in polarized pp collisions.

polarized pp collisions and the dashed line is for $\sqrt{s}=500$ GeV polarized pp collisions. Note that the spin asymmetry is decreased for higher energies. The spin asymmetry for χ_{c1} is for $\lambda=1$ which at LO arises from the color octet contribution from quark-antiquark fusion processes, see eq. (10). For $\sqrt{s}=500$ GeV the spin asymmetry becomes negative in the rapidity range $y \sim 0$ which is due to the polarized quark distribution function at this center of mass energy.

In Fig. 15 we present the rapidity distributions of the longitudinal spin asymmetry A_{LL} for χ_{c2} production in polarized p-p collisions at RHIC. The solid line is for $\sqrt{s}=200$ GeV polarized pp collisions and the dashed line is for $\sqrt{s}=500$ GeV polarized pp collisions. Note that the longitudinal spin asymmetry is decreased for higher energies. The spin asymmetry of χ_{c2} production is almost same for $\lambda=1$ and 0.

One can see from the above figures that the cross sections for the $\lambda = \pm 1$ states dominate over the $\lambda=0$ states. This is explained by the fact that the coefficient in front of the $\langle \mathcal{O}_8^{\chi_{c0}}(^3S_1) \rangle$ term in eqn. (10) in the color octet channel vanishes for $\lambda = 0$. However,

the longitudinal spin asymmetry remains almost same for $\lambda=1$ and $\lambda=0$.

Measurement of $\chi_{cJ}(\lambda)$ polarizations with helicities $\lambda = \pm 1$ and $\lambda=0$ in polarized p-p collisions at RHIC at the PHENIX detector can be useful to test the spin transfer process in pQCD. This will also be useful to extract polarized gluon distribution function inside proton.

IV. CONCLUSIONS

We have studied inclusive χ_{cJ} production with definite polarizations in polarized proton-proton collisions at $\sqrt{s} = 200$ GeV and 500 GeV at RHIC by using non-relativistic QCD (NRQCD) color-octet mechanism. We have presented results of rapidity distribution of χ_{c0} , χ_{c1} and χ_{c2} production with specific polarizations in polarized p-p collisions at RHIC within the PHENIX detector acceptance range. We have also presented the corresponding results for the spin asymmetries.

The PHENIX experiment should be able to measure these spin asymmetries of χ_{cJ} production. The study of heavy quarkonium production with definite helicities in polarized p-p collisions is unique because it tests the spin transfer processes in perturbative QCD. As Tevatron data for heavy quarkonium polarization [24] is not explained by the color octet mechanism [20], the RHIC data may shed some light along this direction.

The measurement of heavy quarkonium production with definite polarization would also provide important information about quark-gluon plasma formation [2] at RHIC and LHC.

-
- [1] V. Ravindran, J. Smith and W. L. van Neerven, Nucl. Phys. B682, 421 (2004), hep-ph/0311314; Nucl. Phys. B647, 275 (2002), hep-ph/0207076 ; Nucl. Phys. Proc. Suppl. 135, 14 (2004), hep-ph/0405233; W. Vogelsang and F. Yuan, hep-ph/0507266; W. Vogelsang, Pramana 63, 1251 (2004), hep-ph/0405069.
- [2] M. Gyulassy and L. McLerran, Nucl. Phys. A750, 30 (2005), nucl-th/0405013; G. C. Nayak, A. Dumitru, L. McLerran and W. Greiner, Nucl. Phys. A687 (2001) 457; F. Cooper, E. Mottola and G. C. Nayak, Phys. Lett. B555 (2003) 181; R. S. Bhalerao and G. C. Nayak, Phys. Rev. C61 (2000) 054907; G. C. Nayak and V. Ravishankar, Phys. Rev. C58 (1998) 356; Phys. Rev. D55 (1997) 6877.

- [3] H. P. Da Costa (for the PHENIX collaboration) "Phenix results for J/ψ production in Au+Au and Cu+Cu collisions at $\sqrt{S_{NN}} = 200$ GeV, proceedings of the Quark Matter conference, August 4-9, (2005), Budapest, Hungary, <http://qm2005.kfki.hu/>; I. Younus, Hawaii DNP2005 APS/JPS meeting.
- [4] N. Brambilla *et al.* (Quarkonium Working Group), hep-ph/0412158, and references therein.
- [5] G. T. Bodwin, E. Braaten and G. P. Lepage, Phys. Rev. D51, 1125 (1995), Erratum-ibid D55, 5853 (1997), hep-ph/9407339.
- [6] G. C. Nayak, J. Qiu and G. Sterman, Phys. Lett. B613 (2005) 45; Phys. Rev. D72 (2005) 114012; Phys. Rev. D74 (2006) 074007; Phys. Rev. Lett. 99 (2007) 212001; Phys. Rev. D77 (2008) 034022.
- [7] ATLAS Collaboration, arXiv:1407.5532 [hep-ex]; CMS Collaboration, Phys. Lett. B727 (2013) 101; LHCb Collaboration, Eur. Phys. C74 (2014) 2835; ALICE Collaboration, Eur. Phys. C74 (2014) 2974; B. Fulson, arXiv:1409.2601 [hep-ex]; LHCb Collaboration, Eur. Phys. C73 (2013) 2631; CMS Collaboration, JHEP02(2012)011; LHCb Collaboration, Eur. Phys. C72 (2012) 2100; ATLAS Collaboration, Phys. Rev. D 87 (2014) 052004; ATLAS Collaboration, arXiv:1404.7035 [hep-ex]; CMS Collaboration, Eur. Phys. C72 (2012) 2251; LHCb Collaboration, JHEP10(2013)115; CMS Collaboration, CMS-PAS-BPH-13-005; F. Adad *et al.* [ATLAS Collaboration], ATLAS Note ATLAS-CONF-2010-062; J. Kirk [ATLAS Collaboration], PoS(ICHEP 2010) 013; V. Khachatryan *et al.* [CMS Collaboration], Eur. Phys. C71 (2011) 1575; E. Scapparini [ALICE Collaboration], Nucl. Phys. B (Proc. Suppl.) 214 (2011) 56; R. Aaij *et al.* [LHCb Collaboration], Eur. Phys. C71 (2011) 1645.
- [8] F. Abe *et al.* [CDF Collaboration], Phys. Rev. Lett. 79 (1997) 572; Phys. Rev. Lett. 79 (1997) 578; Phys. Rev. Lett. 75 (1995) 4358; B. Abbott *et al.* [D0 Collaboration], Phys. Rev. Lett. 82 (1999) 35; T. Affolder *et al.* [CDF Collaboration], Phys. Rev. Lett. 85 (2000) 2886; Phys. Rev. Lett. 86 (2001) 3963; D. Acosta *et al.* [CDF Collaboration], Phys. Rev. Lett. 88 (2002) 161802; Phys. Rev. D 66 (2002) 092001; Phys. Rev. D 71 (2005) 032001.
- [9] E. Braaten and S. Fleming, Phys. Rev. Lett. 74, 3327 (1995), hep-ph/9411365; E. Braaten, S. Fleming and T. C. Yuan, Ann. Rev. Nucl. Part. Sci. 46, 197 (1996), hep-ph/9602374; E. Braaten, S. Fleming and A. K. Leibovich, Phys. Rev. D63, 094006 (2001), hep-ph/0008091.
- [10] P. L. Cho and A. K. Leibovich, Phys. Rev. D53, 6203 (1996), hep-ph/9511315; Phys. Rev. D53, 150 (1996), hep-ph/9505329.

- [11] B. A. Kniehl, G. Kramer and C. P. Palisoc, Phys.Rev. D68 (2003) 114002.
- [12] M. Cacciari and M. Kramer, Phys. Rev. Lett. 76, 4128 (1996), hep-ph/9601276; M. Beneke, M. Kramer and M. Vanttinen, Phys. Rev. D57, 4258 (1998), hep-ph/9709376; J. Amundson, S. Fleming and I. Maksymyk, Phys. Rev. D56, 5844 (1997), hep-ph/9601298; R. M. Goodbole, D. P. Roy and K. Sridhar, Phys. Lett. B373, 328 (1996), hep-ph/9511433; B. A. Kniehl and G. Kramer, Phys. Rev. D56, 5820 (1997), hep-ph/9706369.
- [13] C. G. Boyd, A. K. Leibovich and I. Z. Rothstein, Phys. Rev. D59, 054016 (1999), hep-ph/9810364; M. Klasen, B. A. Kniehl, L. N. Mihaila and M. Steinhauser, Phys. Rev. Lett. 89, 032001 (2002), hep-ph/0112259.
- [14] M. Beneke and I. Z. Rothstein, Phys. Rev. D54, 2005 (1996) [Erratum-ibid. D54, 7082] (1996)], hep-ph/9603400; W. K. Tang and M. Vanttinen, Phys. Rev. D54, 4349 (1996), hep-ph/9603266; S. Gupta and K. Sridhar, Phys. Rev. D54, 5545 (1996), hep-ph/9601349.
- [15] F. Cooper, M. X. Liu and G. C. Nayak, Phys. Rev. Lett. 93 (2004) 171801; G. C. Nayak, M. X. Liu and F. Cooper, Phys. Rev. D68 (2003) 034003.
- [16] M. Klasen, B. A. Kniehl, L. N. Mihaila and M. Steinhauser, Phys. Rev. D68, 034017 (2003), hep-ph/0306080.
- [17] S. Fleming and I. Maksymyk, Phys. Rev. 54 (1996) 3608, hep-ph/9512320.
- [18] S. Gupta and P. Mathews, Phys. Rev. D55, 7144 (1997), hep-ph/9609504; Phys. Rev. D56, 3019 (1997), hep-ph/9703370; Phys. Rev. D56, 7341 (1997), hep-ph/9706541.
- [19] E. Braaten and Y-Q Chen, Phys. Rev. D54, 3216 (1996), hep-ph/9604237.
- [20] E. Braaten, B. A. Kniehl and J. Lee, Phys. Rev. D62, 094005 (2000), hep-ph/9911436; E. Braaten and J. Lee, Phys. Rev. D63, 071501 (2001), hep-ph/0012244; M. Beneke and M. Kraemer, Phys. Rev. D55, 5269 (1997), hep-ph/9611218; A. K. Leibovich, Phys. Rev. D56, 4412 (1997), hep-ph/9610381.
- [21] G. C. Nayak and J. Smith, Phys. Rev. D73 (2006) 014007.
- [22] W. D. Nowak and A. Tkabladze, Phys. Lett. B443 (1998) 379, hep-ph/9809413.
- [23] O. Teryaev and A. Tkabladze, Phys. Rev. D56 (1997) 7331; S. Fleming and T. Mehen, Phys. Rev. D57 (1998) 1846; S. Gupta and P. Mathews, Phys. Rev. D55 (1997) 7144; M. A. Doncheski and R. W. Robinett, Z. Phys. C63 (1994) 611; T. Morii *et al.*, Phys. Lett. B372 (1996) 165.
- [24] T. Affolder, et al, CDF Collaboration, Phys. Rev. Lett. 85, 2886 (2000), hep-ex/0004027.
- [25] J. Babcock, E. Monsay, and D. Sivers, Phys. Rev. D19, 1483 (1979); V. Ravindran, J. Smith

- and W. L. van Neerven, Nucl. Phys. B682, 421 (2004), hep-ph/0311304.
- [26] H. S. Chung, C. Yu, S. Kim and J. Lee, Phys.Rev.D81:014020,2010.
- [27] M. Beneke and M. Krämer, Phys. Rev. D55, 5269 (1997), hep-ph/9611218.
- [28] M. Glück, E. Reya and A. Vogt, Z. Phys. C67, 433 (1995).
- [29] T. Gehrmann and W.J. Stirling, Phys. Rev. D53, 6100 (1996), hep-ph/9512406.
- [30] M. Glück, E. Reya, M. Stratmann and W. Vogelsang, Phys. Rev. D63, 094005 (2001), hep-ph/0011215.
- [31] J. Blumlein and H. Böttcher, Nucl. Phys. B636, 225 (2002), hep-ph/0203155.
- [32] M. Glück, E. Reya and A. Vogt, Euro. Phys. J. C5, 461 (1998), hep-ph/9806404.